Journal of Statistical Physics, Vol. 101, Nos. 1/2, 2000

Selection of an Attractor in a Continuum of Stable Solutions: Descriptions of a Wave Front at Different Scales

A. Lemarchand[1]

Received January 5, 2000

Details of the particle dynamics are shown to modify the mean speed of a chemical wave front propagating into an unstable stationary state. The comparison of several description methods at different scales allows us to discriminate between different sources of departure from the macroscopic deterministic prediction and to give a quantitative expression of the speed corrections induced by discretization of the variables, internal fluctuations in small systems, and departure from local equilibrium in the presence of a fast reaction.

KEY WORDS: Reaction–diffusion system; stochastic description; wave front; nonequilibrium kinetics; microscopic simulations.

1. INTRODUCTION

The paper is devoted to the analysis of a chemical wave front propagating into an unstable stationary state and to the problem of selection of its propagation speed.[1–17] Depending on the scale of the description chosen, the selected speed is different. To put it in a more general frame, the point is to determine the mechanisms governing the selection of a given attractor in a continuum of stable solutions. My motivation is to weave some links between the microscopic description of a spatio-temporal structure and its macroscopic properties. A way to better understand these links is to identify generic situations where the macroscopic deterministic dynamics is sensitive to even weak perturbations and thus, in particular, to the details of the underlying microscopic dynamics. A well-known example of such a sensitive situation is the vicinity of a bifurcation where the amplitude of

[1] Université Pierre et Marie Curie, Laboratoire de Physique Théorique des Liquides, C.N.R.S. U.M.R. 7600, 4 place Jussieu, 75252 Paris Cedex 05, France.

0022-4715/00/1000-0579$18.00/0

fluctuations diverges.[18] But this critical behavior only occurs for specific values of the parameters. A second example is self-organised criticality,[19] where the macroscopic system evolves by itself toward a critical state, this time, in a large domain of parameter values. I am interested here in a third class of generic situations where internal fluctuations can be intuitively suspected of playing a role at an observable scale: It is the case of dynamical systems admitting a continuum of simultaneously stable solutions, easy to be visited by even small fluctuations. The propagation of a wave front into an unstable stationary state offers a simple as well as rich example of this kind of behavior.

To be more specific and in the frame of a macroscopic analysis first, I consider the following partial differential equation for the single continuous variable $a(x, t)$, depending on space x and time t:

$$\partial_t a = ka(1-a) + D\partial_x^2 a \tag{1}$$

For simplicity, the equation is written in the case of a one-dimensional (1d) medium. The dependence of the results on the dimension of the medium is examined at the end of the paper. Depending on the domain of application of the model, the parameters k and D have different physical meanings. Equation (1) admits two homogeneous stationary states, $a=1$, which is stable, and $a=0$, which is unstable. It also admits a continuous family of wave front solutions $a(x, t) = A(x - Ut)$, propagating at a constant speed U. A linear stability analysis in the frame of the wave front proves the stability of the solutions propagating at a speed greater, than the minimum value $U_{\min} = 2\sqrt{kD}$. An essential result of the macroscopic description[3] is that for sufficiently steep initial profiles, like a step function, the minimum velocity $U_{\min}$ is selected: it is the so-called marginal stability criterion. The partial differential equation given in Eq. (1) describes a large variety of phenomena in biology,[20, 21] chemistry, combustion or economy. It has been introduced by Fisher[1] and Kolmogorov, Petrovsky, and Piskunov[2] (KPP) in the frame of population dynamics to model the propagation of a favored gene A in a constant population of A and B. In the following, I use the same model to describe the propagation of a wave in a chemical inhomogeneous medium. The parameter D is thus interpreted as the diffusion coefficient of the chemical species A and B, susceptible to react according to the autocatalytic reaction

$$\mathrm{A} + \mathrm{B} \rightarrow 2\mathrm{A} \tag{2}$$

If the total concentration C of species A and B is initially homogeneous, it remains constant for any position x and time t, and the macroscopic

deterministic evolution of the local fraction $a(x, t)$ of particles A obeys Eq. (1) with $k = KC$ where K is the rate constant of reaction (2).

As already mentioned, the point is to examine if the results of the macroscopic deterministic description are robust when the underlying microscopic dynamics of the particles is taken into account. This analysis may be performed at different scales and my goal here is to compare the results given by different approaches performed in collaboration with Michel Mareschal and Bogdan Nowakowski. The different methods used are briefly recalled in Section 2. The details of the procedures followed to solve the equations or to perform numerical simulations may be found elsewhere. The results are compared in Section 3, and the corrections to front speed induced by discretization of the variables, internal fluctuations, and departure from local equilibrium are calculated. The possible dependence of the results on the medium dimension is analyzed at the end of Section 3. The conclusions are given in Section 4.

2. DIFFERENT LEVELS OF DESCRIPTIONS

The reaction-diffusion model associated with the macroscopic equation given by Eq. (1) can be described at an intermediate level using a master equation approach.[18, 22, 23] In this stochastic description, the details of the microscopic dynamics are not accessible but their effect is expressed, at a mesoscopic level, by internal fluctuations of the variables. Contrary to the deterministic description by Eq. (1), the master equation involves discrete variables, the numbers $N_A(i)$ and $N_B(i)$ of particles A and B in each spatial cell i of length Δx. For Fisher-KPP model, the master equation[16] governing the probability P reads:

$$
\begin{aligned}
d_t P(\{N_A(i), N_B(i)\}) &= \sum_i \left\{ \frac{k}{N} [(N_A(i)-1)(N_B(i)+1)\, P(N_A(i)-1, N_B(i)+1) \right. \\
&\quad - N_A(i)\, N_B(i)\, P] + \frac{D}{(\Delta x)^2} [(N_A(i)+1)(P(N_A(i)+1, N_A(i+1)-1) \\
&\quad + P(N_A(i-1)-1, N_A(i)+1)) - 2N_A(i)\, P \\
&\quad + (N_B(i)+1)(P(N_B(i)+1, N_B(i+1)-1) \\
&\quad \left. + P(N_B(i-1)-1, N_B(i)+1)) - 2N_B(i)\, P] \right\} \qquad (3)
\end{aligned}
$$

where N is the mean number of particles in a cell and where the dependence of P on particle numbers has been omitted in the right hand side if it does not differ from those of the left hand side. We have followed two different ways to solve the master equation. The first method[16] consists in directly simulating the master equation using the Monte Carlo method introduced by Gillespie.[24] The main steps of the procedure are recalled in the Appendix. In the second method,[7, 8] the master equation is replaced by approximate equations of Langevin type using the following hypotheses:[23] Switching to continuous variables, the fluctuating local fractions of particles, $\alpha = N_A(i)/N$ and $\beta = N_B(i)/N$, the master equation is expanded in power of $1/N$ according to the so-called system-size expansion,[22] and the probability is assumed to be Gaussian. According to these assumptions, the problem reduces to solving stochastic partial differential equations: the effect of the underlying microscopic dynamics is reproduced by adding Langevin forces F_α and F_β to the deterministic equations for the local fractions of particles A and B. It reads:

$$\partial_t \alpha = k\alpha\beta + D\partial_x^2 \alpha + F_\alpha \tag{4}$$

$$\partial_t \beta = -k\alpha\beta + D\partial_x^2 \beta + F_\beta \tag{5}$$

The mean and variance of the Langevin forces are supposed to define on their own the whole statistics. At dominant order they are given by[8, 23]

$$\langle F_\alpha \rangle = \langle F_\beta \rangle = 0$$

$$\langle F_\alpha(x, t)\, F_\alpha(x', t') \rangle = \frac{\delta(t-t')}{N} \left\{ ka(1-a)\, \delta(x-x') + 2D \frac{\partial^2}{\partial x\, \partial x'} [\, a\delta(x-x')\,] \right\}$$

$$\langle F_\beta(x, t)\, F_\beta(x', t') \rangle = \frac{\delta(t-t')}{N} \left\{ ka(1-a)\, \delta(x-x') + 2D \frac{\partial^2}{\partial x\, \partial x'} [\, (1-a)\, \delta(x-x')\,] \right\}$$

$$\langle F_\alpha(x, t)\, F_\beta(x', t') \rangle = -\frac{\delta(t-t')}{N} ka(1-a)\, \delta(x-x') \tag{6}$$

where the local fraction a of particles A obeys the deterministic equation (1). The Langevin equations are then solved numerically[8] on a CRAY supercomputer.

To obtain information at a more microscopic level, one has to follow the evolution of the position and impulsion of each particle. Reliable

statistics on the mean propagation speed of a spatio-temporal structure like a wave front are not easily accessible from Molecular Dynamics (MD) simulations. Instead of MD, we have used an efficient simulation method introduced by Bird[25] which proposes a Monte Carlo treatment of collisions between particles in a same spatial cell. The simulation can be regarded as a direct simulation of the Boltzmann equation for the distribution $f_A(x, \mathbf{v}, t)$ of the positions and velocities of particles A. Following Bird,[25] we consider a dilute gas of hard spheres of diameter d and mass m whatever their chemical species. The medium is divided into linearly arranged cells of length Δx equal to a fraction of the mean free path λ. According to the main assumption, we consider that each cell is homogeneous. During the simulation time step Δt chosen as a fraction of the mean free time, the free motion of particles and their mutual collisions are supposed to be uncoupled. Particle velocities are treated in three dimensions, but their positions are projected on the direction of front propagation, and the perpendicular coordinates are disregarded. In these conditions, the section of the cells and consequently the number density are adjustable parameters and the dilute gas assumption is not restrictive. The results presented have been obtained for the following parameter values: density $C = 0.1$, temperature $k_B T = 1$, mass $m = 1$, and diameter $d = 1$.

The collisions are performed in 3d as follows. A collision between a pair (i, j) of particles randomly chosen in a same cell is accepted if their relative speed obeys:

$$|\mathbf{v}_i - \mathbf{v}_j| > R v^r_{\max} \tag{7}$$

where $0 \leqslant R \leqslant 1$ is a random number and $v^r_{\max}$ is a continuously updated maximum relative speed. A collision impact parameter is chosen randomly and the postcollisional velocities are deduced from the energy and impulsion conservation laws. A cell time variable is increased by an evaluation of the approach time of the colliding pair and next collisions are performed untill the cell time reaches Δt. In this paper the reaction is supposed to have a vanishing activation energy and each collision can be reactive with the same probability s_f, corresponding to a steric factor. The case of an activated reaction is treated in ref. 15. At small s_f, the simulation results for rate constant k coincide with the value obtained under the assumption of equilibrium for the velocity distribution:[25]

$$k = 4Cd^2 \sqrt{\frac{\pi k_B T}{m}}\, s_f \tag{8}$$

where C is density.

In addition, we have looked for an approximate analytical solution of the Boltzmann equation for the distribution $f_A(x, \mathbf{v}, t)$ of the positions and velocities of particles A:

$$\partial_t f_A + v_x \partial_x f_A = \int (f_A(\mathbf{v}')\, f_A(\mathbf{v}_1') - f_A(\mathbf{v})\, f_A(\mathbf{v}_1))\, |\mathbf{v} - \mathbf{v}_1|\, d\sigma_{AA}\, d\mathbf{v}_1$$

$$+ \int (f_A(\mathbf{v}')\, f_B(\mathbf{v}_1') - f_A(\mathbf{v})\, f_B(\mathbf{v}_1))\, |\mathbf{v} - \mathbf{v}_1|\, d\sigma_{AB}\, d\mathbf{v}_1$$

$$+ \int f_A(\mathbf{v}')\, f_B(\mathbf{v}_1')\, |\mathbf{v} - \mathbf{v}_1|\, d\sigma_{AB}^*\, d\mathbf{v}_1 \tag{9}$$

where v_x is the projection of particle velocity along the x-axis, σ_{AA} and σ_{AB} are the cross sections for elastic collisions of hard spheres A–A and A–B, respectively, and σ_{AB}^* is the cross section for reaction (2). Only velocities are indicated explicitly as arguments of the distributions in the collision integrals, and the primes denote postcollisional velocities. The isothermal reaction (2) which only changes the chemical identity of molecules does not affect the velocity distribution of the mixture as a whole. Consequently, the initial mechanical equilibrium of the whole system is maintained all the time. It means that:

$$f_A + f_B = C \exp\left(-\frac{mv^2}{2k_B T}\right) \tag{10}$$

so that Eq. (9) involves only the distribution function of A. To solve analytically the Boltzmann equation (9), we use the Chapman–Enskog method,[26–29] applied to inhomogeneous reactive systems. In this perturbative approach, it is assumed that the chemical process as well as the transport process can be treated as perturbations.[30, 31] Explicit results of our analytical approach can be found in ref. 15.

Irrespective of the level of description adopted to study the wave front, the initial profile chosen is sufficiently steep to obey the conditions of selection of the minimum velocity, $U_{\min}$, found in the frame of a macroscopic analysis.[3] Whatever the method chosen, the same type of boundary conditions are imposed, first, to mimic an infinite medium, and second, to switch into a frame moving with the front. To compute the fluctuating propagation speed, the idea is to follow the total number of particles A in the system. Then, a time average of this speed is determined. For example, the initial and boundary conditions chosen in the case of the microscopic

simulations are the following. Initially, particles A are located in the cells of the left half, and particles B in the cells of the right half of the medium. When the total number of particles A becomes greater than its initial value, the first left cell becomes the last right one while its particles A are transformed into B's, and the front position $\phi(t)$ is increased by Δx. Provided the length of the simulated medium is sufficiently large (about ten times the front width) both the particles A on the extreme left and the particles B on the extreme right have equilibrium velocity distributions,[15] allowing us to change their chemical nature if necessary. For the parameter values chosen, this trick is actually performed only about every 100th time step on average. It amounts to switching into a frame moving with speed $U(t)$, equal to the time derivative of $\phi(t)$, appearing as the fluctuating front speed. Independently of the microscopic realization of the initial condition (reducing at a macroscopic level to a step function), the time average of the local fraction of particles A in the moving frame evolves to a stationary profile and the moving frame reaches a stationary mean speed $\langle U \rangle$.

As summarized in Table I, mean propagation speeds, different from the minimum speed, $U_{\min}$, are observed when solving the Langevin equations, the master equation, the Boltzmann equation, and when performing microscopic simulations using Bird's method: One observes three effects of different nature, leading all to a speed correction with respect to the prediction of the macroscopic description.

Table I. Corrections to the Minimum Propagation Speed $U_{\min}$ Induces by Different Types of Perturbations with Respect to the Deterministic Macroscopic Description. The Results Are Deduced from the Comparison of Several Methods of Description of Different Scales. The Presence of an X in a Cell Means that the Method Used Takes into Account the Mentioned Perturbation

	Discretization of the variables	Fluctuation of the variables	Departure from local equilibrium
Langevin equations		X	
Master equation	X	X	
Microscopic simulations	X	X	X
Boltzmann equation			X
Consequences on mean front speed	$U_{\min} - \langle U \rangle \propto (\ln(N))^{-2}$ $N \gg 10^8$ Refs. 12, 13	$\langle U \rangle - U_{\min} \propto N^{-1/3}$ $N < 10^4$ Refs. 7, 8, 10, 16	$\langle U \rangle = U'_{\min} = 2\sqrt{k'D'}$ Refs. 14–16

3. COMPARISON OF THE RESULTS GIVEN BY THE DIFFERENT METHODS

3.1. Effect on Wave Front Speed of the Discretization of the Variables

When dealing with discrete variables, a speed decrease with respect to $U_{\min}$ is observed. This effect has been interpreted in the frame of a macroscopic description by Brunet and Derrida[12] which have introduced a small cutoff in the nonlinear reactive term of the partial differential equation given in Eq. (1). In a microscopic simulation, $1/N$, where N is the mean number of particles in a spatial cell, plays the role of an effective cutoff. Actually, one can see $1/N$ as the height of a small jump in the leading edge of the front, due to the presence of the first A particle in a sea of B's. Since the analysis[3] of the partial differential equation given in Eq. (1) has revealed the crucial role played by the shape of the leading edge in the speed selection problem, the determining role of a cutoff can be intuitively suspected. Brunet and Derrida[12] have shown that the presence of a cutoff decreases the front speed according to the following logarithmic law

$$\frac{U_{\min} - \langle U \rangle}{U_{\min}} = \frac{\pi^2}{2(\ln(N))^2} \tag{11}$$

According to Eq. (11), the effect of discretization only disappears for very large values of N. It is well-known when performing MD simulations in standard, noncritical situations, that a set of hundred molecules already have macroscopic properties in average. In the case of a wave front propagating into an unstable state, or more generally, when the dynamical system admits a continuum of stable solutions, corrections to the macroscopic limit are observable even for $N = 10^{15}$ particles per cell.[12] They should be detectable in experiments involving small systems.

3.2. Effect on Wave Front Speed of Internal Fluctuations

Independently of the discretization of the variables, one observes an other effect which cannot be explained in the frame of a purely deterministic description. This second effect is isolated in the approach using Langevin equations for continuous variables: It can be attributed to internal fluctuations. We have shown[7, 8] that the numerical integration of the Langevin equations associated with Fisher-KPP model leads to an increase of the front speed according to a power law with a small exponent equal to 1/3. The effect of fluctuations is also present in the results deduced from

the master equation[16] and from microscopic simulations using Bird's method,[16] but it is superimposed to the effect of the discretization of the variables. Figure 1 shows the deviations from Brunet and Derrida prediction[12] given in Eq. (11). These deviations are observed when solving the master equation by Gillespie method[24] and performing microscopic simulations using Bird's method[25] in a domain of small N, obeying $N < 10^4$. These two independent descriptions prove that a positive correction to speed, due to internal fluctuations, is added to the negative correction

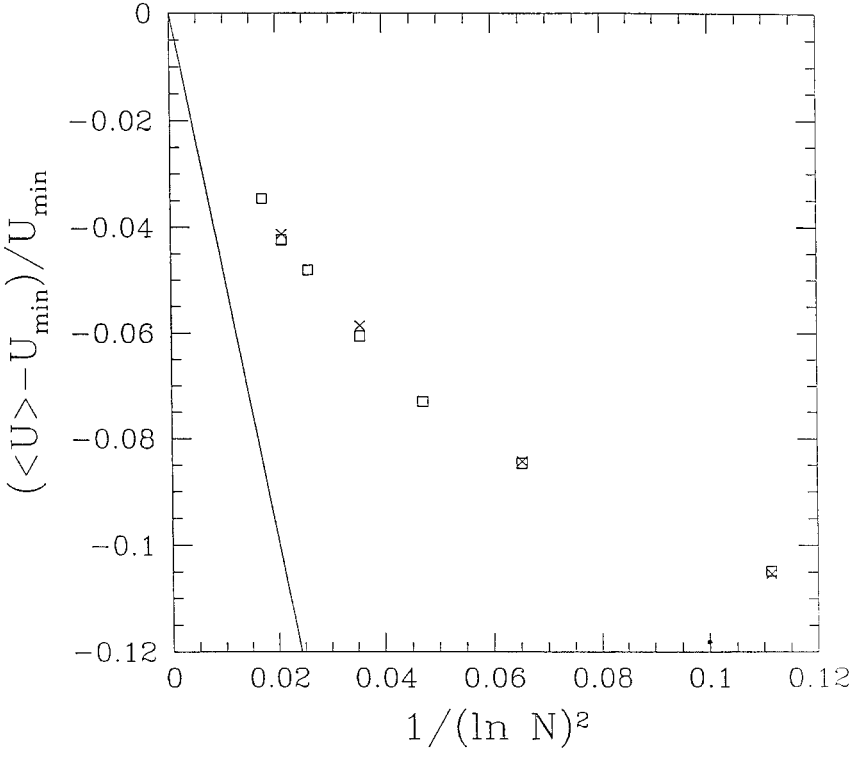

Fig. 1. Effect on wave front speed of the discrete number N of particles in a cell: relative deviation from $U_{\min}$ of the time averaged front propagation speed versus $1/(\ln(N))^2$. The crosses are results of microscopic simulations using Bird's method (steric factor $s_f = \exp(-1.5)$, number of simulated cells $n_x = 800$, cell length $\Delta x = E_{\min}/79 = \lambda/6$ where λ is the mean free path and where $E_{\min}$ is the macroscopic prediction for the front profile width). The open squares are results given by the master equation (number of simulated cells $n_x = 512$, cell length $\Delta x = E_{\min}/64$). The line with a slope of $-\pi^2/2$ corresponds to the prediction of Brunet and Derrida when a cutoff is introduced in the deterministic equation.

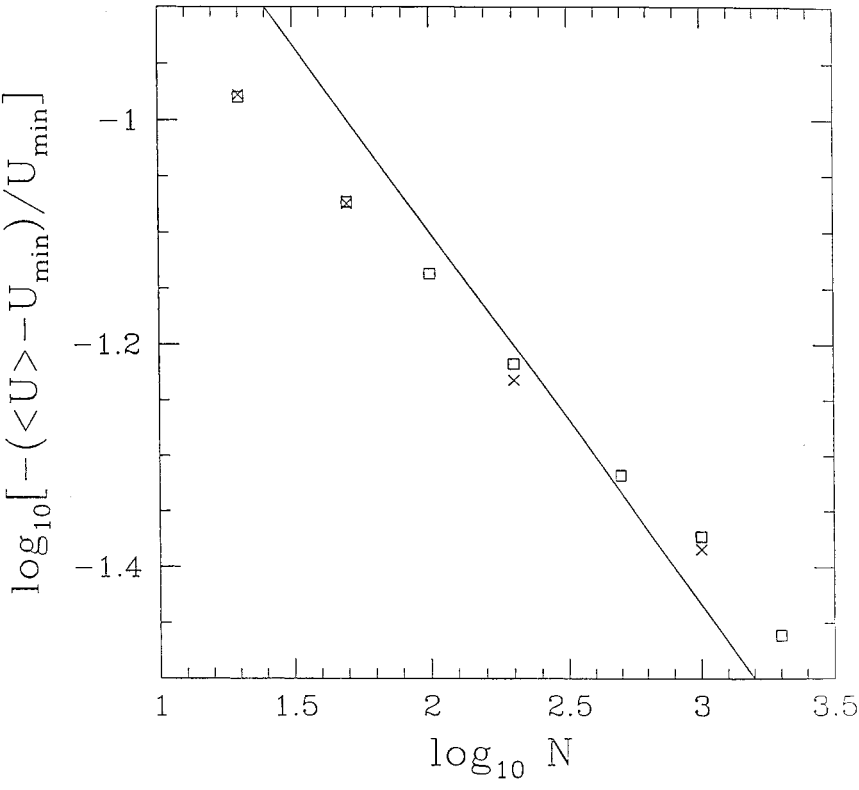

Fig. 2. Effect on wave front speed of the internal fluctuations: $\log_{10}-\log_{10}$ plot of the opposite of the relative deviation from $U_{\min}$ of the time averaged front propagation speed versus mean number N of particles in a cell. Crosses and open squares correspond to the same results as in Fig. 1. The line with a slope of $-1/3$ is obtained when solving the Langevin equations for continuous variables (the local fractions).

induced by the discretization of the variables. Using in Fig. 2 a log–log plot for the same results, reveals the following power law:

$$\frac{\langle U\rangle - U_{\min}}{U_{\min}} \sim N^{-\gamma} \tag{12}$$

where the exponent $\gamma = 0.24 \pm 0.02$ is close to 1/3.

These results should answer the question raised in the literature[7–10, 12, 13] about the existence of a power law or a logarithmic correction to the front speed: we conclude that both exist, but the power law given in Eq. (12) cannot be neglected in the domain of small N ($N < 10^4$) whereas the

logarithmic correction given in Eq. (11) prevails at large N. On the one hand, the very good agreement between master equation and microscopic simulation results given in Fig. 1 in the range $N \leqslant 10^4$, and, on the other hand, the noticeable decrease of the deviation between these results and the logarithmic prediction as N increases and tends to 10^4 make the conclusion quite reasonable.

Because of obvious computational costs, the microscopic simulation results cannot be obtained for enormous values of N so that they are significantly affected by internal fluctuations and discretization effects. However, if one performs microscopic simulations in order to study the actual macroscopic properties of a system, the effects of internal fluctuations and those induced by the discretization of the variables can be seen as artifacts, which vanish in the macroscopic limit.

3.3. Effect on Wave Front Speed of a Departure from Local Equilibrium

The results given by the microscopic simulations à la Bird exhibit a third effect on wave front speed, only detectable in approaches which give access to the velocity distribution of the particles. This third effect, which remains unchanged in the macroscopic limit, is induced by a perturbation of the local equilibrium observed when the chemical reaction is fast.[26, 27] Actually, if the characteristic time between two reactive collisions is not large enough compared to the time between elastic collisions, the particle velocity distribution does not have time to relaxe toward the equilibrium distribution at temperature T between two successive perturbations by the chemical reaction. Even if the reaction does not have an activation energy, the results of the microscopic simulations given in Fig. 3 show that the particles A have a higher kinetic energy, i.e., a higher temperature in the front zone. In the same way, the particles B have a lower temperature in this region since the total kinetic energy is conserved. The effect of chemical reaction (2) does not only result in an increase of the effective temperature of particles A but also in a deviation from the Maxwellian character of the particle velocity distribution. As shown in Fig. 3, the departure from the Gaussian shape is characterized in the front zone by nonvanishing values of the kurtosis κ_{yz} restricted to coordinates y and z

$$\kappa_{yz} = \left(\frac{m}{2k_B T}\right)^2 (\langle (v_y{}^2 + v_z{}^2)^2 \rangle - 2\langle v_y{}^2 + v_z{}^2 \rangle^2) \tag{13}$$

Here v_y and v_z are the particle velocity components along y- and z-axis. In the Monte Carlo procedure adopted by Bird[25] and in agreement with

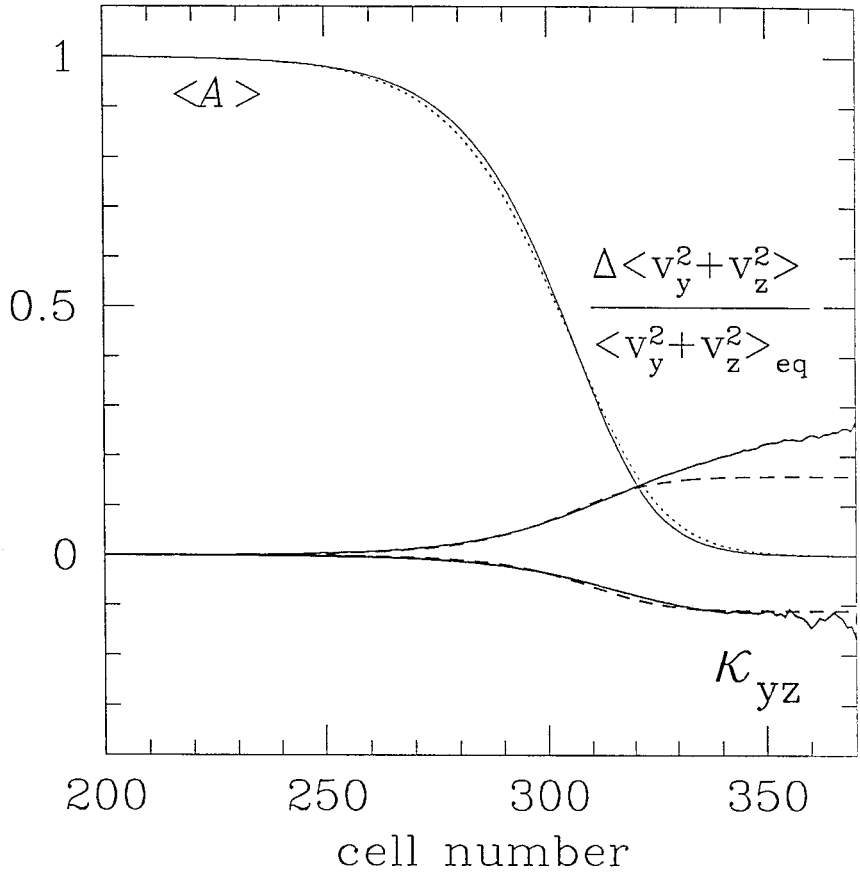

Fig. 3. Departure from local equilibrium in the leading edge of the front: spatial variations in the moving frame of the kurtosis κ_{yz} of the A particle velocity distribution, of the relative deviation of its second moment $\langle v_y{}^2 + v_z{}^2 \rangle$ to its equilibrium value $2k_B T/m$, and comparison of time averaged local fraction $\langle A \rangle$ of particles A (solid line) with the corresponding deterministic profile propagating with the minimum velocity $U_{\min}$ (short-dashed line). Solid (resp. long-dashed) lines correspond to microscopic simulations (resp. analytical, based on the Boltzmann equation) results. The reaction has a vanishing activation energy, the steric factor equals $s_f = \exp(-0.5)$, the mean number of particles in a cell is $N = 1000$.

the expression of the collision integral in the Boltzmann equation, a collision, however elastic or reactive it is, is accepted if the relative speed of the colliding pair is sufficient. Considering again the autocatalytic scheme given in Eq. (2), one sees that a collision between a particle A and a particle B will be most likely accepted if A and B are both fast so that the two A's, which will be created in case of reaction, will also be most likely fast. It is

therefore not surprising to observe an increase of the kinetic energy of particles A at the reactive interface between particles A and B. This effect is detectable for large steric factors and disappears[15] as the reaction becomes slow, for $s_f < \exp(-7)$. From a macroscopic point of view, an important consequence of the deformation of the particle velocity distribution is the modification of reaction rate constants[26, 27] and transport coefficients.[30–32] Admitting that the marginal stability criterion[3] is valid, the front speed deduced from the Boltzmann equation reads

$$U = 2\sqrt{k'D'} \tag{14}$$

where k' and D' are respectively the rate constant and the diffusion coefficient deduced from the second order perturbation solution[15] of the Boltzmann equation. The explicit expression of k' and D' can be found in ref. 15. At first sight, the results deduced from Boltzmann equation and from the microscopic simulations do not coincide in Fig. 4. As recalled in Table I, the front speed correction deduced from Boltzmann equation is only due to nonequilibrium effects whereas the microscopic simulations lead to the superposition of three independent effects—discretization of the variables, internal fluctuations, and nonequilibrium effects. At small steric factors $s_f < \exp(-3)$, i.e., for sufficiently slow reactions, nonequilibrium effects on front speed become negligible and microscopic simulation results agree with master equation results: In this range of steric factors, the simulation results only account for discretization and fluctuation effects. Hence, their comparison with the results deduced from Boltzmann equation simply requires a translation along the ordinate axis until the asymptotic values at small s_f coincide. Now, the agreement is much better. Note however that the speed correction deduced from the perturbative approach of the Boltzmann equation is not reliable at very large values of s_f, when the perturbation of the distribution by the chemical reaction becomes too important. For values of s_f close to 1, the approximate analytical approach overestimates the speed correction.

3.4. Do the Results Depend on the Dimension of the Medium?

The results of the previous sections have been obtained in a 1d-medium, essentially to limit the computational costs. The efficiency of the numerical integration of the Langevin type equations given in Eqs. (5) allowed us to compare the results obtained in 1d-, 2d- and 3d-media: At this scale of description, the mean velocity of the front does not depend on the dimension of the medium.[7] The paper of Riordan *et al.*[5] incited us to determine if the time variation of the front position variance depends on the dimension

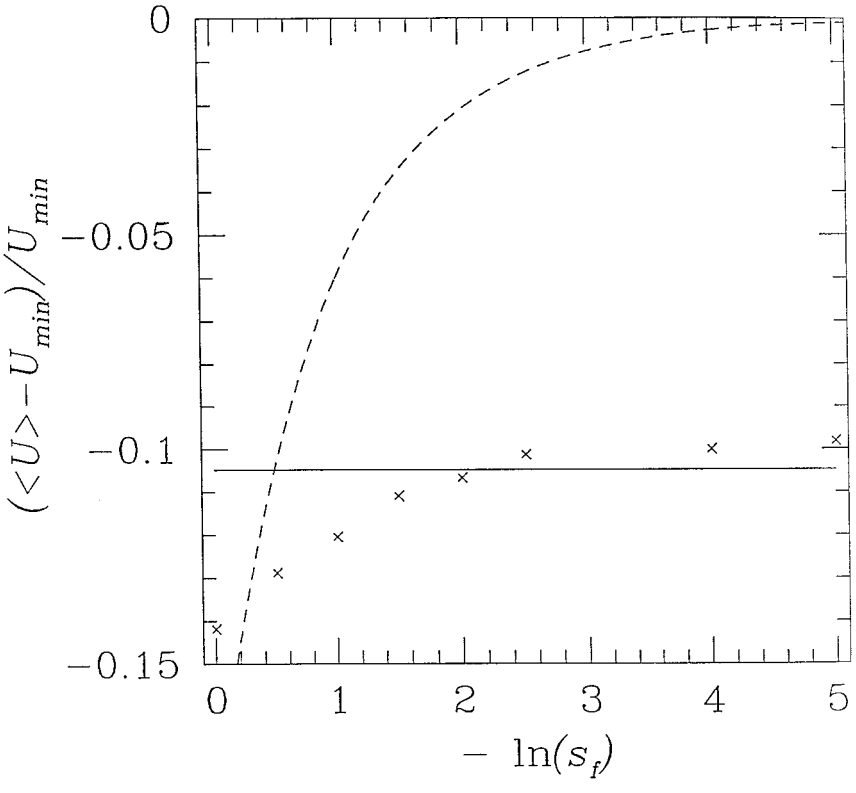

Fig. 4. Effect on wave front speed of the perturbation of local equilibrium by a nonactivated reaction: relative deviations from $U_{\min}$ of the time averaged front propagation speed versus steric factor s_f (in logarithmic units). The crosses correspond to the results of microscopic simulations using Bird's method: The mean number of particles in a cell is fixed to $N = 20$, the cell length, Δx, varies with s_f in order to impose $E_{\min}/\Delta x = 64$. The dashed curve is deduced from a perturbative solution of the Boltzmann equation. The straight (solid) line is the result given by the master equation for $N = 20$ and $E_{\min}/\Delta x = 64$.

of the medium. Using Monte Carlo simulations on a lattice, Riordan *et al.*[5] observe that in a 2d-medium, the front position does not have a diffusive motion: They observe an increase of the front position variance as $t^{0.54}$ instead of t. Figures 5 and 6 give the evolution of position variance determined from an ensemble average, after integration of Langevin type equations for a large number of different realizations of the same macroscopic initial condition. As shown in Fig. 5, the choice of very steep initial conditions corresponding at a macroscopic level to a step function, induces the existence of a transient regime with a nondiffusive front position

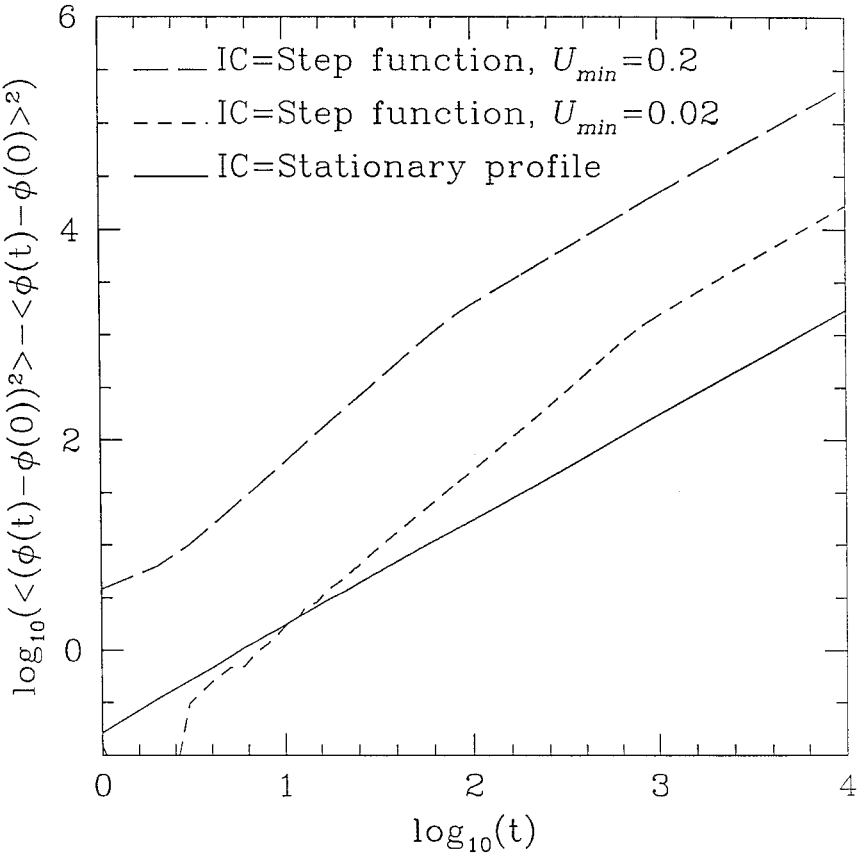

Fig. 5. Log–log plot of the variance of front position $\phi(t)$ versus time for different types of initial conditions (IC) or different minimum propagation speeds $U_{\min}$. The Langevin equations associated with Fisher model are solved numerically in a 2d-medium of 110×64 cells for the following parameter values $k = D = U_{\min}/2$, $N = 1000$. In each case, the statistics is performed over 20 different realizations of the same type of initial conditions.

motion which is replaced at large time by the classical spreading. If we choose as initial conditions different realizations of the profile, which is stationary in the moving frame, a diffusive motion is observed from the very beginning, irrespective of the medium dimension, as shown in Fig. 6. There are two main differences between the approach of Riordan *et al.*[5] and ours. The first point is that Riordan *et al.* consider the reversible model $A + A \rightleftharpoons A$ whereas we deal with the irreversible Fisher model given in Eq. (2). Both models lead to the same macroscopic deterministic equation but to different mesoscopic and microscopic properties. The second point

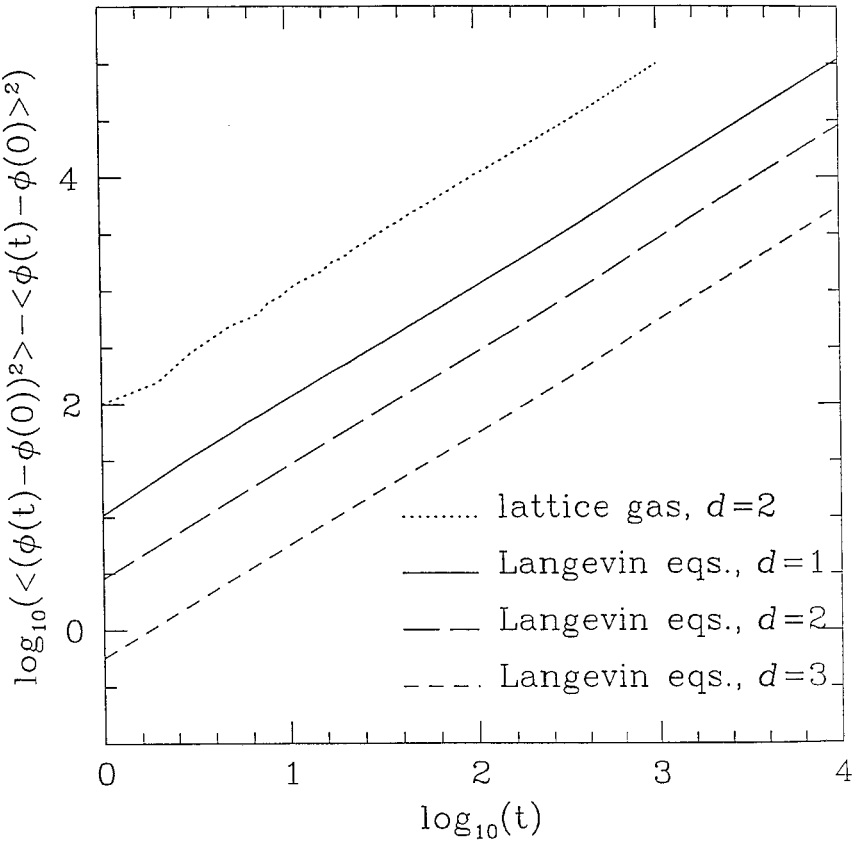

Fig. 6. Log–log plot of the variance of front position $\phi(t)$ versus time in a 1d-, 2d-, or 3d medium. In each case, the statistics is performed over 20 different realizations of the stationary profile in the moving frame. The Langevin equations associated with Fisher model are solved numerically for the parameter values $k = D = 0.1$, $N = 1000$ in a 1d-medium of 110 cells, in a 2d-medium of 110×64 cells, and in a 3d-medium of $110 \times 64 \times 64$ cells. The result are compared with 2d-lattice-gas simulations of HPP type. The curves have been arbitrarily shifted to avoid superposition.

is that reaction is limited by diffusion in ref. 5 whereas rate constant k and diffusion coefficient D are independent in our case. This second point reveals as being important and may explain the observed difference of behaviors with respect to the dependence on medium dimension.

As shown in Fig. 6, our results deduced from Langevin type equations are confirmed by the simulations we performed on a 2d-reactive lattice gas cellular automaton[33] of Hardy, de Pazzis, and Pomeau (HPP) type.[34] We are aware that obtaining the same power laws using the Langevin

equations and other independent methods does not necessarily validate the explicit expressions of the Langevin forces F_α and F_β used in Eq. (5). It simply proves that some, essential properties of the fluctuating dynamics are included in the equations we used. It is not sufficient to legitimate the system-size expansion of the master equation. Using Poisson representation[23, 25] or renormalization group method[36] should allow us to determine if we used proper internal noise expressions.

4. CONCLUSIONS

The propagation of a wave front into an unstable state offers a generic example of situations where the macroscopic properties of the system are influenced by the details of the particle dynamics. To analyze their consequences on mean wave front speed, resorting to microscopic simulations is therefore essential. The results deduced from microscopic simulations à la Bird[25] allow us to observe effects of different origins: The front speed varies, for example, with the mean number N of particles simulated in a spatial cell and with the frequency of the reactive collisions. Nevertheless, the vast amount of information included in the microscopic simulation results is hardly exploitable alone. It turns out that the comparison of several approaches, at different scales, is necessary to discriminate between the different sources of disagreement with the prediction of the deterministic theory. Keeping a macroscopic description level, Brunet and Derrida[12] prove that the introduction of a small cutoff in the nonlinear term of the partial differential equation gives account for the dependence of the simulation results on N, for large N: the front speed is decreased by the discretization of the variables according to the following logarithmic law

$$\frac{U_{\min} - \langle U \rangle}{U_{\min}} = \frac{\pi^2}{2(\ln(N))^2}, \qquad N \gg 10^8$$

At a mesoscopic level, the Langevin approach allows us to isolate the effect of internal fluctuations and to prove that they increase the mean wave front speed as

$$\frac{\langle U \rangle - U_{\min}}{U_{\min}} \sim N^{-1/3}, \qquad N < 10^4 \tag{15}$$

As shown by the direct simulation of the master equation and by the microscopic simulation, the logarithmic law induced by discretization dominates at large N whereas the fluctuation effect can be detected at small N. The analytical approach based on the Boltzmann equation enables us to

isolate the effects of a fast chemical reaction and to prove that the decrease of the front speed, observed in microscopic simulations for frequent reactive collisions, is due to a departure from local equilibrium. Three distinct effects, discretization of the variables, internal fluctuations, and perturbation of particle velocity distribution have been shown to modify the mean front speed. This unusual sensitivity is related to the existence of a continuum of stable wave front solutions. Actually, it is to be noted that a trigger wave, propagating with a uniquely defined speed between two stable stationary states has completely different properties. Using Langevin equations, we have shown[8] that the internal fluctuations also increase the speed of this type of front, but their effect dies as $N^{-3/2}$. An analogous power law with the same value of the exponent has been found[13] when introducing a cutoff $1/N$ in the chemical term of the partial differential equation. The trigger wave therefore appears as a good candidate for the analysis of the only effects of departure from local equilibrium on the front speed. Work in this direction is in progress.[37]

APPENDIX. GILLESPIE METHOD

We use the Monte Carlo (MC) method introduced by Gillespie[24] to directly simulate the master equation (3). To determine a new configuration $\{N_A(i), N_B(i)\}$ at each time step, it is necessary to choose appropriately the following random variables: (i) a waiting time τ for the next event, (ii) a cell in which the event occurs, and (iii) the type of the event (reaction or diffusion). For a Markovian process, the probability distribution of τ is exponential and given by $\nu_{\text{tot}} \exp(-\nu_{\text{tot}}\tau)$. Here $\nu_{\text{tot}} = \sum_i \nu(i)$ is the total rate of all the processes in the system, i.e., the sum of the rates $\nu(i)$ of the processes occuring in each cell i. Thus, at point (ii) an index i of a cell in which the next event occurs is chosen with the probability $\nu(i)/\nu_{\text{tot}}$. The rate $\nu(i)$ depends on the problem considered and its explicit form follows from the transition rates involved in the corresponding master equation. According to Eq. (3) for the Fisher wave front, the rate of the processes in the ith cell is $\nu(i) = kN_A(i)\, N_B(i)/N + 2(D/(\Delta x)^2)(N_A(i) + N_B(i))$. Having determined a cell number i, a process of a given type is chosen at point (iii) with a probability proportional to the contribution of its rate to $\nu(i)$. For example, the probability of reaction is $kN_A(i)\, N_B(i)/(N\nu(i))$ and the probability of diffusion for a A particle to jump to the left or the right adjacent cell is given by $(D/(\Delta x)^2)\, N_A(i)/\nu(i)$. We generate the random evolution of the system in a single time step by choosing τ, i and a type of process according to the given above probabilities following from the configuration $\{N_A(i), N_B(i)\}$ at that time. Time is increased by τ and the populations $\{N_A(i), N_B(i)\}$ are updated according to the chosen process.

ACKNOWLEDGMENTS

I would like to thank Bernard Derrida, Charlie Doering, Michel Droz, and Zoltan Racz for their suggestions.

REFERENCES

1. R. A. Fisher, *Ann. Eugenics* **7**:335 (1937).
2. A. Kolmogorov, I. Petrovsky, and N. Piskunov, *Bull. Univ. Moscow. Ser. Int. Sec. A* **1**:1 (1937).
3. D. G. Aronson and H. F. Weinberger, *Adv. Math.* **30**:33 (1978); W. van Saarloos, *Phys. Rev. Lett.* **58**:2571 (1987); W. van Saarloos, *Phys. Rev. A* **37**:211 (1988); W. van Saarloos, *Phys. Rev. A* **39**:6367 (1989).
4. S. Cornell, M. Droz, and B. Chopard, *Phys. Rev. A* **44**:4826 (1991); B. Chopard, M. Droz, T. Karapiperis, and Z. Racz, *Phys. Rev. E* **47**:R40 (1993).
5. J. Riordan, C. R. Doering, and D. ben-Avraham, *Phys. Rev. Lett.* **75**:565 (1995).
6. H.-P. Breuer, W. Huber, and F. Petruccione, *Physica D* **73**:259 (1994); *ibid.*, *Europhys. Lett.* **30**:69 (1995).
7. A. Lemarchand, A. Lesne, and M. Mareschal, *Phys. Rev. E* **51**:4457 (1995).
8. M. Karzazi, A. Lemarchand, and M. Mareschal, *Phys. Rev. E* **54**:4888 (1996).
9. Ch. Dellago and H. A. Posch, *Physica A* **240**:68 (1997).
10. R. van Zon, H. van Beijeren, and Ch. Dellago, *Phys. Rev. Lett.* **80**:2035 (1998).
11. J. Mai, I. M. Sokolov, and A. Blumen, *Europhys. Lett.* **44**:7 (1998).
12. E. Brunet and B. Derrida, *Phys. Rev. E* **56**:2597 (1997).
13. D. A. Kessler, Z. Ner, and L. M. Sander, *Phys. Rev. E* **58**:107 (1998).
14. A. Lemarchand and B. Nowakowski, *Europhys. Lett.* **41**:455 (1998).
15. A. Lemarchand and B. Nowakowski, *J. Chem. Phys.* **109**:7028 (1998).
16. A. Lemarchand and B. Nowakowski, *J. Chem. Phys.* **111**:6190 (1999).
17. M. Velikanov and R. Kapral, *J. Chem. Phys.* **110**:109 (1999).
18. G. Nicolis and I. Prigogine, *Self-Organization in Nonequilibrium Systems* (Wiley, New York, 1977).
19. P. Bak, C. Tang, and K. Wiesenfeld, *Phys. Rev. Lett.* **59**:381 (1987).
20. J. D. Murray, *Mathematical Biology* (Springer, Berlin, 1989).
21. A. J. Koch and H. Meinhardt, *Rev. Mod. Phys.* **66**:1481 (1994).
22. N. G. van Kampen, *Stochastic Processes in Physics and Chemistry* (North-Holland, Amsterdam, 1977).
23. C. W. Gardiner, *Handbook of Stochastic Methods* (Springer, Berlin, 1985).
24. D. T. Gillespie, *J. Comput. Phys.* **22**:403 (1976).
25. G. A. Bird, *Molecular Gas Dynamics* (Clarendon, Oxford, 1976).
26. I. Prigogine and E. Xhrouet, *Physica* **15**:913 (1949).
27. B. Shizgal and M. Karplus, *J. Chem. Phys.* **52**:4262 (1970); *ibid.* **54**:4345 and 4357 (1971).
28. S. Chapman and T. G. Cowling, *The Mathematical Theory of Nonuniform Gases* (Cambridge University Press, London, 1953).
29. D. Napier and B. Shizgal, *Phys. Rev. E* **52**:3797 (1995); B. Shizgal and D. Napier, *Physica A* **223**:50 (1996).
30. B. Nowakowski and J. Popielawski, *J. Chem. Phys.* **100**:7602 (1994).
31. B. V. Alexeev, A. Chikhaoui, and I. T. Grushin, *Phys. Rev. E* **49**:2809 (1994).
32. B. Nowakowski and A. Lemarchand, *J. Chem. Phys.* **106**:3965 (1997).

33. A. Lemarchand, I. Nainville, and M. Mareschal, *Europhys. Lett.* **36**:227 (1996).
34. J. Hardy, O. de Pazzis, and Y. Pomeau, *Phys. Rev. A* **13**:1949 (1976).
35. M. Droz and A. McKane, *J. Phys. A* **27**:L467 (1994).
36. P.-A. Rey and M. Droz, *J. Phys. A* **30**:1101 (1997).
37. A. Lemarchand and B. Nowakowski, *Physica A* **271**:87 (1999).